

STRUCTURAL INVESTIGATIONS OF SNOW AND ICE ON CORE III FROM THE DRILLING ON VERNAGTFERNER, AUSTRIA, IN 1979

By WALTER GOOD, Davos

With 8 figures and 12 pictures

ABSTRACT

The purpose of this study was:

- To make an attempt at finding a stratification of the snowpack in order to help remove ambiguities in dating the snowlayers by standard methods.
- To verify the depth at which the transition between firn and ice occurs.

Clearly the first goal was missed, the structural information in a temperate firn being strongly smoothed out in time.

Interesting details like horizontal ice lenses and layers of "cold snow" however, were revealed.

In spite of strong variations of density, gravimetric density ρ_G and ice density ρ_i , computed from point density, are identical for the firn pack between $Z=2.0$ m and 6.0 m.

$$\rho(\text{ice}) = 0.522 \pm 0.034 \cdot 10^3 \text{ kg m}^{-3}.$$

The ice density of $0.8 \cdot 10^3 \text{ kg m}^{-3}$, the assumed transition between firn and ice, was found to occur at a depth of $Z=19$ m. Even at this level, rather important variations in density may be localized. Between $Z=19$ m and 21 m, the ice density varies from $0.774 \cdot 10^3$ to $0.860 \cdot 10^3 \text{ kg m}^{-3}$.

STRUKTURANALYSEN AN SCHNEE- UND EISPROBEN DER KERNBOHRUNG III AUF DEM VERNAGTFERNER (ÖSTERREICH) AUS DEM JAHRE 1979

ZUSAMMENFASSUNG

Zweck dieser Untersuchung war,

- einen Versuch zu unternehmen, den schichtweisen Aufbau der Firnauflage zu erkennen, um Zweideutigkeiten in der zeitlichen Einordnung nach Standardmethoden auszuschließen,
- die Tiefe zu bestimmen, in der sich der Übergang von Firn in Eis vollzieht.

Das erste Ziel wurde eindeutig verfehlt. Die strukturellen Informationen im temperierten Firn werden mit der Zeit stark verwischt. Es wurden jedoch interessante Details, wie horizontale Eislinsen und Schichten von „kaltem Schnee“, erkannt.

Trotz großer Schwankungen bei der Dichte sind die gravimetrisch bestimmten Dichten ρ_G und die aus der Punktdichte berechneten Eisdichten ρ_i für die Firnschicht zwischen 2,0 und 6,0 m gleich groß:

$$\rho(\text{ice}) = 0,522 \pm 0,034 \cdot 10^3 \text{ kg m}^{-3}.$$

Die Eisdichte von $0,8 \cdot 10^3 \text{ kg m}^{-3}$, die für den Übergang von Firn zu Eis veranschlagt wird, wurde in einer Tiefe von $Z=19$ m vorgefunden. Merklliche Dichteschwankungen konnten selbst

noch in diesem Tiefenbereich festgestellt werden. Zwischen $Z=19$ m und 21 m variierte die Eisdichte in einem Bereich von $0,774 \cdot 10^3$ bis $0,860 \cdot 10^3 \text{ kg m}^{-3}$.

1. PREPARATION OF SNOW SAMPLES

The core from drilling III, located at an altitude of 3150 m a.s.l., from 2./3. 4. 1979, was packed and cooled down to dry ice temperature after careful measuring and photographing its individual parts (Oerter et al., 1982).

The samples were then forwarded to Davos, Switzerland, where they were embedded in an organic liquid to become, in its frozen state, a matrix to prevent any subsequent alteration (phthalic acid diethyl ester).

In spite of this proven conservation technique, changes in the snow structure were found as can be observed on unprotected samples stored for extended periods even at temperatures below -20°C .

Two reasons for these alterations are most probable, the time elapsed between drilling and embedding and the high density snow ($\sim 0,5 \cdot 10^3 \text{ kg m}^{-3}$) where not all pores are easily attained by the filler liquid. The unprotected pores are then exposed to temperature gradient metamorphism.

The preparation of thin sections started with visual inspection of the core for homogeneous domains, where cubes of $3 \times 3 \times 3 \text{ cm}^3$ were cut out. Vertical slices were cut and honed on a microtome to a final thickness of $20 \pm 1 \mu\text{m}$. Dyed tetralin dissolved the organic matrix leaving clear ice particles separated by a colored liquid phase. With a WILD photomicroscope, high quality color photographs were taken for each thin section.

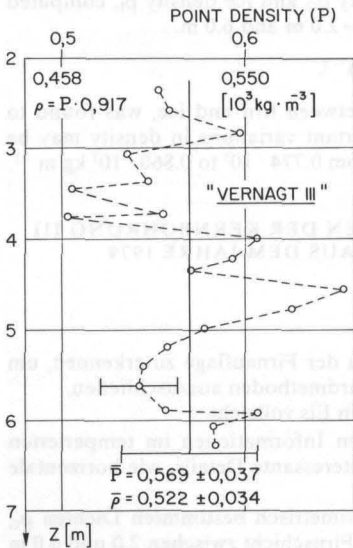


Fig. 1

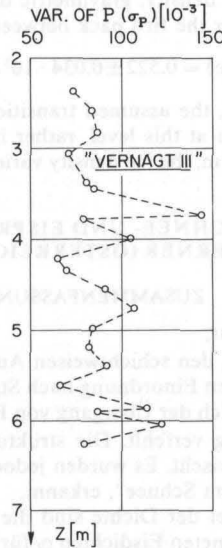


Fig. 2

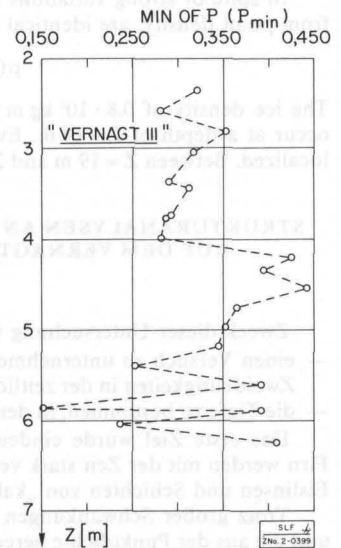


Fig. 3

Fig. 1: Vernagtferner core III: Point density (P) and ice density (ρ) for samples between $Z=2$ m and 6 m taken over 512×512 pixels. — Fig. 2: Core III: Variance of point density (σ_P) for samples between $Z=2$ m and 6 m. — Fig. 3: Core III: Minimum of point density (P_{\min}) for samples between $Z=2$ m and 6 m

2. STRUCTURAL EVALUATION BY IMAGE ANALYSING TECHNIQUES

The photographic information of thin sections is transmitted to a dec pdp 11/45 computer via a HAMAMATSU slow scan video camera. Analog/digital conversion and control is performed with a C-1000 HAMAMATSU interface and the digital data are accepted through DR-11 parallel interface. The software controlling these operations and storing data on magnetic tape is MVIDAD. In normal operation mode, an image of a thin section is represented by 512×512 pixels. This information may be processed in either or both of two ways (Good, 1980):

- Pattern sampling technique (S).
- Pattern recognition technique (fig. 8 [P]; pict. 9).

For the actual study, the first sampling technique was used (Underwood, 1970).

2.1 PARAMETER GENERATION

The program MVIDHIS reads the picture row by row from the storage tape (512 pixels) and evaluates, among other parameters,

- Point density (P), the number of sampling points falling on ice particles over the total number of pixels.
- Line intersects (P_L), the number of transitions void-ice and ice-void over the number of pixels per line.
- The grain intercept lengths (L_L^G), the distances between void-ice and ice-void transitions.

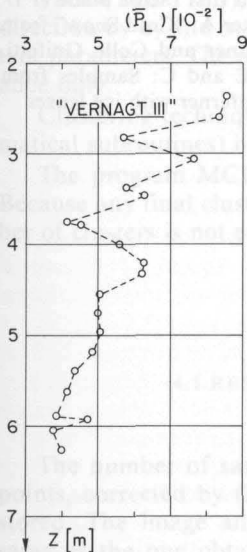


Fig. 4

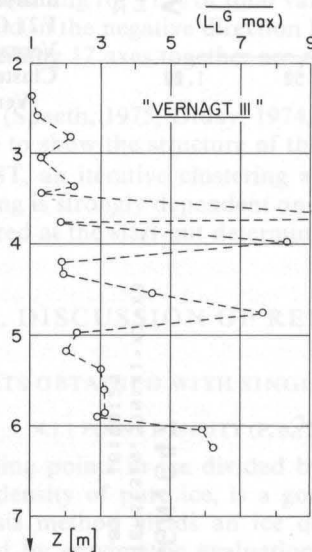


Fig. 5

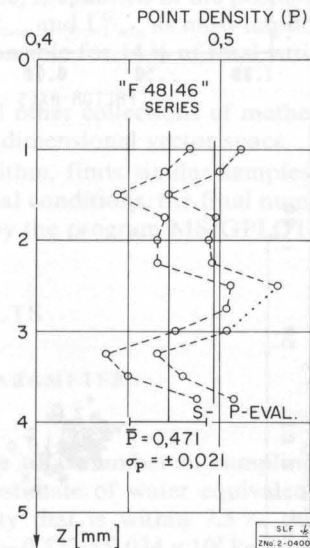


Fig. 8

Fig. 4: Vernagtferner core III: Mean line intersects (\bar{P}_L) for samples between $Z=2$ m and 6 m. The average is taken over 512 scanning lines. — Fig. 5: Vernagtferner core III: Mean maximum line intercept length ($\bar{L}_{L,max}^G$) for samples between $Z=2$ m and 6 m. The average is taken over 512 scanning lines. — Fig. 8: Weissfluhjoch: 12 Serial cuts from one sample of "Summer Snow" spaced $250 \mu\text{m}$. Point density (P) for S- and P-evaluation is given

— The void intercept lengths (L_v^y), the distance between ice-void and void-ice transitions.

The corresponding parameter distributions per line and over all lines (512) are computed. Thus a set of over 20 parameters (mean, variance, minimum, and maximum) and characteristic for each snow sample is generated.

Point density P (or the derived ice density), for instance, proves to be a very poor

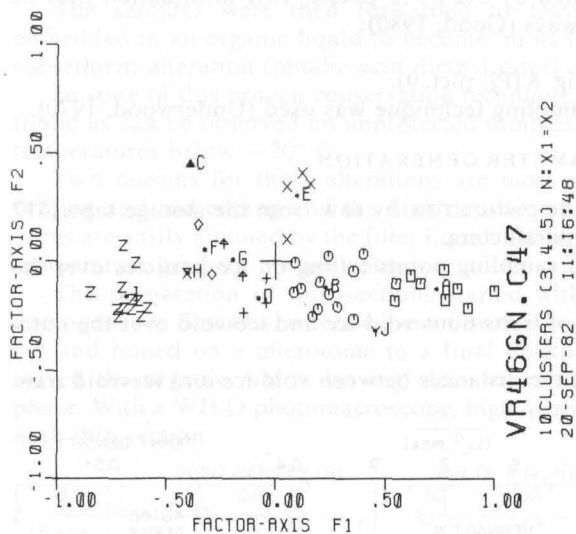


Fig. 6: Vernagtferner core III, Colle Gnifetti: Result of multivariate analysis in first factor plane (F1/F2). Cluster A: "Cold Snow" from Vernagtferner and Colle Gnifetti. Clusters E and C: Samples from Vernagtferner with ice lenses

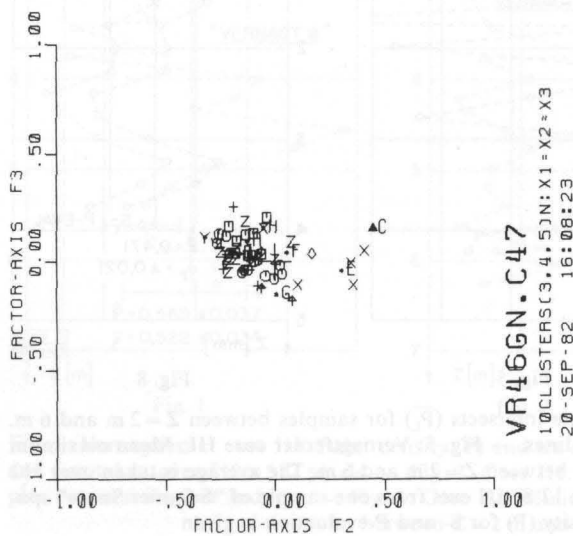


Fig. 7: Vernagtferner core III, Colle Gnifetti: Result of multivariate analysis in second factor plane (F2/F3). Same scale as figure 6. Increasing point density is in direction of F2 (Clusters C, E)

structural parameter, whereas the mean maximum line (grain) intercept length ($\overline{L_{L_{\max}}^G}$) easily reveals the samples with ice layers in the horizontal (scanning) direction (fig. 1, 5).

A more complete discussion of the discriminant power of single parameters is given in section 4.1.

3. MULTIVARIATE DATA ANALYSIS

The $n=47$ analyzed snow samples span a $p=20$ (parameters) dimensional vector space. The discussion of similitude or dissimilitude of samples is simplified when choosing an orthogonal vector space. Here, Euclidian distances may be defined to describe "differences" between samples.

The technique of factorial analysis (Cooley et al., 1973, Lebart and Fenelon, 1973, and other collections of mathematical subroutines) defines mutually orthogonal axes by selecting appropriate linear combinations of the p parameters (MFACTOR). Their importance decreases in the following order:

Factor axis 1 (F1), carrying 50 % of total variance, is spanned in the positive direction mainly by P_L and $P_{L_{\max}}$ whereas in the negative direction the most important parameters are L_L^G , L_L^V and σL_L^V .

Factor axis 2 (F2), increasing the variance by an additional 25 %, is spanned in the positive direction by point density (P , P_{\max}).

Factor axis 3 (F3), accounting for 11 % of total variance, is spanned in the positive direction by σ_p and σ_{P_L} , and in the negative direction by P_{\min} and $L_{L_{\min}}^G$ as most important parameters. The remaining 17 axes together are responsible for 14 % of total variance only.

Clustering techniques (Spaeth, 1975, Diday, 1974, and other collections of mathematical subroutines) have to show the structure of this p -dimensional vector space.

The program MCLUST, an iterative clustering algorithm, finds similar samples. Because any final clustering is strongly dependent on initial conditions, the final number of clusters is not entered at the start but determined by the program MSIGPLOT.

4. DISCUSSION OF RESULTS

4.1 RESULTS OBTAINED WITH SINGLE PARAMETERS

4.1.1 POINT DENSITY (P , σ_p , P_{\min})

The number of sampling points in ice divided by the total number of sampling points, corrected by the density of pure ice, is a good estimate of water equivalent stored. The image analysis method yields an ice density that is within 7.5 ‰ the same as the one obtained by gravimetric evaluation ($\rho_I = 0.522 \pm 0.034 \times 10^3 \text{ kg m}^{-3}$, fig. 1).

Unfortunately, the structural information in this parameter is quasi null. For instance an individual at $Z=2.35 \text{ m}$ and a disturbed sample at $Z=5.87 \text{ m}$ show the same density (Appendix table 1, pict. 1, pict. 8).

The same holds true for the variance of point density (σ_p). There is one individual, however, emerging from the noisy curve, i. e. the one with the most important horizon-

tal ice layer, located at $Z=3.73$ m (pict. 3). The minimum of point density (P_{\min}) has its lowest value with the damaged sample from a depth of $Z=5.87$ m (pict. 8).

Except for really extreme samples, the density does not help any further in classifying the snow samples.

4.1.2 STEREOLOGICAL PARAMETERS

Two examples, one with a rather smooth curve (mean line intersects \overline{P}_L , fig. 4) and the other with sharp peaks (mean, maximum line intercept length $\overline{L}_{L_{\max}}^G$, fig. 5) are discussed.

The steady decrease in the number of void-ice, ice-void transitions, a kind of grain coarsening with increasing depth, is exemplified in fig. 4. The three samples with more than 7 transitions per 100 pixels represent the fine grained snow we would like to call "cold snow".

Like all the other sampling parameters, the line intercept length (L_L^G) is computed on a per line basis. Here, the maximum for each line is evaluated and the mean over all 512 lines computed. The mean maximum line intercept length (fig. 5) is a rough approximation of grain diameter. This parameter sharply points out the four samples with ice lenses located respectively at $Z=3.73$ m, 3.98 m, 4.54 m, 4.75 m, and the coarse grained snow around 6 m.

4.2 MULTIPARAMETER DISCUSSION

Fig. 6 displays, in the first factor plane (F1/F2), with the first axis normalized to one, and fig. 7, in the second factor plane (F2/F3), scaled to F1, the distribution of individuals in 10 clusters.

The cluster algorithm in program MCLUST was asked to produce stable configurations grouping all individuals in 3, 4, and 5 clusters respectively. From N runs, given configurations are found n_3 times for three clusters ($n_3/N=.82$), n_4 times for four clusters ($n_4/N=1.0$), and n_5 times for five clusters ($n_5/N=.82$). These are the most frequently occurring configurations and therefore considered to be stable. The intersection of these three stable situations yields the 10 clusters of fig. 6 and 7.

Intersection emphasizes single individuals with peculiar characteristics like the individual of cluster C, with largest ice lenses, the disturbed sample of cluster H ($Z=5.87$ m) and the transition individual of cluster J that deserves a special discussion (see sect. 4.3).

The three firn/ice samples from $Z=19.17$ m (pict. 10), 21.48 m, and 22.75 m (pict. 11) would be way out of the upper left corner in the F1/F2 diagram (see sect. 3). In order to show the complexity and the variability of the analyzed snow samples, the individuals nearest to their respective center of cluster are given as illustrative pictures (pict. 1, . . . 9). They are computer outputs of the corresponding thin sections and represent, by their 512×512 pixels, an area of roughly 2×2 cm². Ice is black and voids are white.

4.3 COMPARISON OF SAMPLES FROM VERNAGTFERNER AND COLLE GNIFETTI

In a previous study (Schotterer et al., 1978), given samples from Colle Gnifetti, Monte Rosa, Switzerland, at an altitude of 4450 m a. s. l., could be identified to stem from snow layers deposited in winter and having not undergone subsequent melt-freeze metamorphism. These samples (pict. 1.1) easily fit in the same factorial

space and are located at the extreme right of cluster A. This suggests similar conditions for the three samples at $Z=2.35$ m, 2.57 m, and 3.04 m, whereas the sample from 2.81 m is easily rejected into cluster B. In fact, individual GNI28 (cluster J) seems to mark the transition between "cold snow" and snow that has undergone firnification processes. Meltwater must have been present, at least partially, in the "cold snow" layer on Vernagtferner, however. In the sample from $Z=2.35$ m (pict. 1), a "percolation path" (ice stalk [Oerter, 1981, p. 9]) is visible near the left border.

4.4 COMPARISON OF SAMPLES FROM VERNAGTFERNER WITH LATE SPRING FIRN

One cluster was left out in the discussion so far, the 12 individuals forming cluster I. The samples were taken at the testsite on Weissfluhjoch/Davos, Switzerland, at an altitude of 2600 m a. s. l. on June 10, 1981. It is a late spring snow having undergone several melt-freeze cycles in the firnification process (pict. 9).

The density of these samples and the size of the grains are comparable to the ones of the sample from $Z=5.61$ m of cluster G (pict. 7).

The differences lie in the shape and the complexity (topology) of the grains. In the samples from cluster G, besides the rounded grains, grains bounded by sharp edges and plane faces are present. The latter might be artifacts as stated previously (see sect. 1) and due to closed pores not protected by the organic filler.

Besides this comparison of shape, the representativity of thin sections from coarse grained snow was tested. 12 serial cuts, spaced 250 μm , were prepared from the same snow sample. The very close gathering of all 12 individuals in cluster I (fig. 6) and the shape of density curve (fig. 8) confirm the feasibility of a comparative study. The variance in point density for several samples from the same spot of the snowcover is therefore estimated to be half the variance of all samples analysed. One such sample point is tentatively reported in fig. 1 for the individual at $Z=5.61$ m.

5. CONCLUSION

Temperate firn does not reveal a stratification that may be found by geometric analyses. Anomalies, strongly shape related characteristics, and artefacts, however, are detectable by image analyzing procedures and careful numerical treatment of the results. One of these anomalies, the "cold snow" type layer with the samples at $Z=2.35$ m, 2.57 m, and 3.04 m might be of snow from winter 1977/78 and protected by the subsequent snowfalls during the cold and wet summer 1978. (In fact, the snow cover lasted on the testsite Weissfluhjoch until August 7, 1978, the latest date for the last 40 years.)

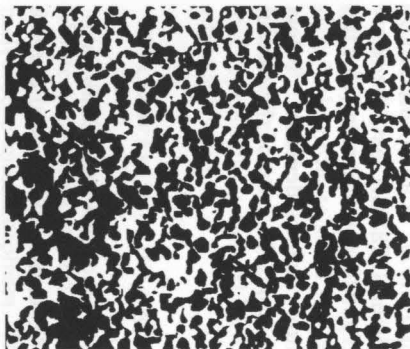
The immersion technique, developed for snow with densities below $0.4 \times 10^3 \text{ kg m}^{-3}$, is not able to fully protect firn or ice samples. In spite of the careful analysis, some results may have a slight bias.

ACKNOWLEDGEMENTS

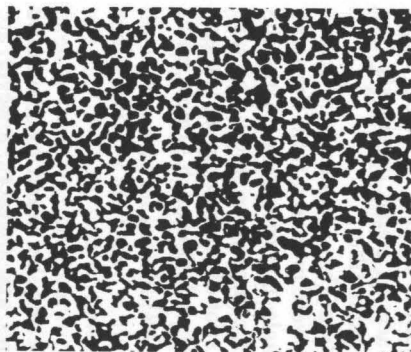
This study was possible thanks to the snow samples provided by:

- Physikalisches Institut der Universität Bern (Colle Gnifetti),
- Institut für Radiohydrometrie der Gesellschaft für Strahlen- und Umweltforschung mbH, München (Vernagtferner).

The very careful preparation of the thin sections is due to G. Kruesi, Swiss Federal Institute for Snow and Avalanche Research, Weissfluhjoch.



Pict. 1



Pict. 1.1

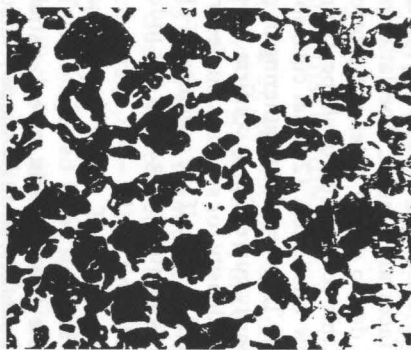


Pict. 2

Pict. 1: Vernagtferner core III: Snow layer from between $Z=2.350$ m and 2.375 m. "Cold Snow" type belonging to cluster A. — Pict. 1.1: Colle Gnifetti: Sample GNI22 from Winter 1975/76 of type "Cold Snow" of cluster A. — Pict. 2: Vernagtferner core III: Snow layer from between $Z=3.360$ m and 3.385 m. Individual from cluster B, representing first stage in firnification



Pict. 3

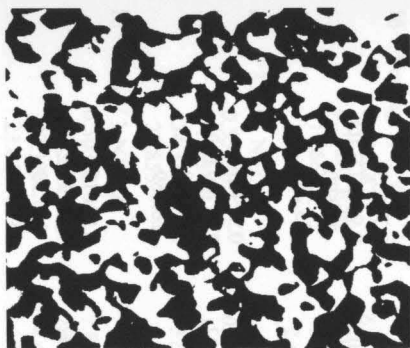


Pict. 4



Pict. 5

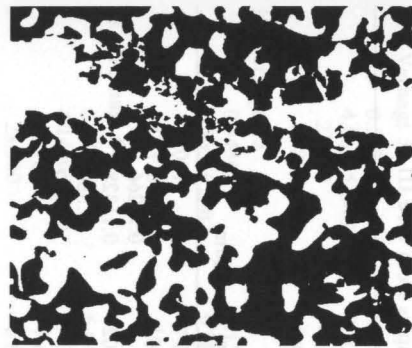
Pict. 3: Vernagtferner core III: Snow layer from between $Z=3.730$ m and 3.755 m. Individual from cluster C with big ice lense. — Pict. 4: Colle Gnifetti: Individuals from cluster D show signs of temperature gradient metamorphism. — Pict. 5: Vernagtferner core III: Snow layer from between $Z=3.980$ m and 4.005 m. Individual from cluster E with small ice lenses



Pict. 6

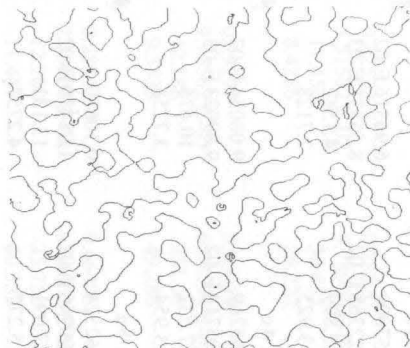


Pict. 7

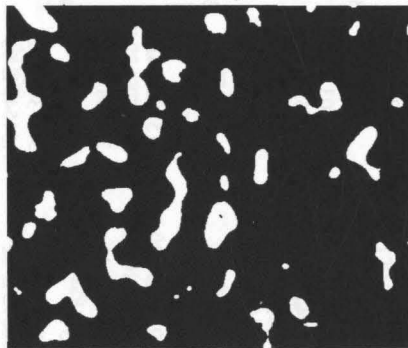


Pict. 8

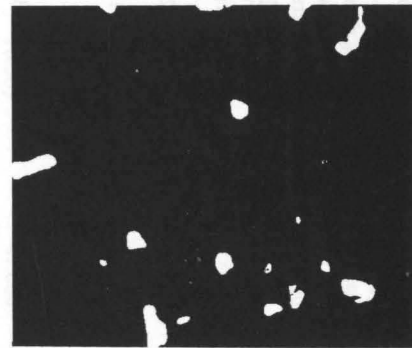
Pict. 6: Vernagtferner core III: Snow layer from between $Z=5.390$ m and 5.415 m. Individuals with largest grains. Cluster F. — Pict. 7: Vernagtferner core III: Snow layer from between $Z=5.610$ m and 5.635 m. Individuals with largest grains. Cluster G. — Pict. 8: Vernagtferner core III: Snow layer from $Z=5.87$ m. Disturbed sample from cluster H



Pict. 9



Pict. 10



Pict. 11

Pict. 9: Weissfluhjoch: "Summer Snow" Circumferences of homogeneous grain areas evaluated via pattern recognition from cluster I. — Pict. 10: Vernagtferner core III: Firn/Ice transition at $Z=19.17$ m. $\rho_i=0.774 \times 10^3 \text{ kg} \cdot \text{m}^{-3}$. — Pict. 11: Vernagtferner core III: Ice at $Z=21.48$ m. $\rho_i=0.860 \times 10^3 \text{ kg} \cdot \text{m}^{-3}$

Table 1: Vernagtferner: Parameters of 21 samples from core III

		Line 1: Label, depth Z in m			
		Line 2: Point density			
		Line 3: Line intersects			
		Line 4: Grain intercept length			
		Line 5: Void intercept length			
Rows:		Mean, variance, minimum, maximum			
1	Vernagt 1 b			2.35	
		0.55167	7.35456 E-02	0.32227	0.72266
		8.57010 E-02	9.57007 E-03	6.05469 E-02	0.11328
		12.983	2.3538	7.4615	19.889
		10.644	2.2003	6.0417	21.250
2	Vernagt 2 c			3.36	
		0.54661	8.08035 E-02	0.29102	0.74414
		5.80940 E-02	8.10766 E-03	3.12500 E-02	8.59375 E-02
		19.191	3.9976	10.294	43.250
		15.931	3.8761	7.8235	30.250
3	Vernagt 3 a			3.43	
		0.50497	8.49703 E-02	0.31250	0.67383
		6.31142 E-02	9.89751 E-03	3.90625 E-02	9.57031 E-02
		16.090	2.6473	10.565	24.909
		16.385	4.7389	8.7895	30.500
4	Vernagt 3 c			3.98	
		0.60580	0.10525	0.38281	0.93750
		5.59387 E-02	1.15590 E-02	1.17187 E-02	8.39844 E-02
		25.114	20.879	11.211	160.00
		14.183	3.2431	6.5000	25.700
5	Vernagt 5 b			4.97	
		0.57712	8.43730 E-02	0.35352	0.76367
		5.06592 E-02	7.64540 E-03	3.32031 E-02	8.00781 E-02
		23.609	5.1656	13.176	45.000
		16.924	4.6235	8.0625	36.778
6	Vernagt 4 b			4.33	
		0.57009	6.96316 E-02	0.39648	0.73633
		6.22368 E-02	8.55838 E-03	3.90625 E-02	8.98437 E-02
		18.899	4.1542	11.783	37.600
		13.925	2.7128	7.5789	23.231
7	Vernagt 4 c			4.54	
		0.65269	9.08054 E-02	0.44336	0.92969
		5.05714 E-02	9.89023 E-03	1.95312 E-02	7.61719 E-02
		27.532	10.475	14.474	86.400
		13.954	3.7258	5.0000	26.889
8	Vernagt 5 a			4.75	
		0.62524	0.10680	0.36719	0.91016
		5.00946 E-02	1.03410 E-02	1.36719 E-02	7.61719 E-02
		27.091	13.131	12.500	147.33
		15.277	4.2757	5.3000	31.900

9	Vernagt 5 c		5.18	
	0.55738	8.21524 E-02	0.34570	0.73242
	4.86145 E-02	7.50342 E-03	2.92969 E-02	6.83594 E-02
	23.298	4.0814	15.706	39.000
	18.857	5.4723	10.250	41.000
10	Vernagt 6 a		5.39	
	0.54369	9.15857 E-02	0.25391	0.79883
	4.36516 E-02	9.18637 E-03	1.17187 E-02	6.83594 E-02
	26.081	7.2405	12.333	58.000
	22.328	10.197	9.7500	125.00
11	Vernagt 6 b		5.61	
	0.54206	6.64795 E-02	0.39258	0.72266
	4.14505 E-02	8.40031 E-03	1.95312 E-02	7.03125 E-02
	27.147	7.4773	15.111	59.800
	23.500	6.8205	10.563	47.000
12	Vernagt 7 b		6.26	
	0.58291	7.88109 E-02	0.41016	0.76953
	4.03061 E-02	6.55307 E-03	1.36719 E-02	5.85937 E-02
	29.955	7.4216	17.200	120.00
	21.262	5.8639	10.333	40.429
13	Vernagt 1 c		2.57	
	0.55832	8.43047 E-02	0.28125	0.77930
	8.37784 E-02	1.04736 E-02	4.29687 E-02	0.11133
	13.419	2.4508	8.2105	23.143
	10.862	3.2329	5.8571	33.091
14	Vernagt 2 a		2.81	
	0.59691	8.71364 E-02	0.35352	0.80273
	5.72281 E-02	8.47423 E-03	2.73437 E-02	8.39844 E-02
	21.287	5.1047	9.5455	41.222
	14.498	3.9164	7.5000	35.429
15	Vernagt 7 a		6.05	
	0.58195	0.12209	0.23828	0.89062
	3.78494 E-02	8.12285 E-03	1.17187 E-02	6.64062 E-02
	32.322	13.849	13.200	114.00
	23.562	9.2947	7.8000	59.000
16	Vernagt 4 a, V4		4.20	
	0.59284	6.47056 E-02	0.42578	0.78320
	6.28281 E-02	1.07740 E-02	3.51562 E-02	8.78906 E-02
	19.666	5.1304	11.450	36.455
	13.248	2.6976	8.4286	26.222
17	F3 BV2 NEG6		3.73	
	0.55530	0.14366	0.29297	0.90039
	4.15611 E-02	1.17223 E-02	9.76562 E-03	6.83594 E-02
	34.332	32.611	12.188	221.00
	21.855	7.2925	9.3333	49.286
18	F3 BV3 NEG8		3.76	
	0.50328	7.86871 E-02	0.28711	0.66405
	4.54597 E-02	7.60731 E-03	2.53906 E-02	6.64062 E-02
	22.384	4.4287	12.200	35.750
	23.011	6.7237	11.467	60.333

19	F6CV2 NEG 1		5.87		
	0.55634	0.11417		0.15234	0.77148
	3.85742 E-02	9.91395 E-03		1.56250 E-02	7.42187 E-02
	30.201	8.3813		9.3333	60.400
	25.448	13.848		11.789	107.75
20	F6CV3 NEG 1		5.90		
	0.60746	8.72063 E-02		0.39258	0.79883
	4.72450 E-02	8.18882 E-03		2.73437 E-02	7.22656 E-02
	26.911	6.6370		13.733	56.000
	16.923	4.6288		7.9231	32.556
21	F2BV2 NEG 1		3.04		
	0.53530	7.06453 E-02		0.31836	0.73242
	7.67479 E-02	8.47544 E-03		4.88281 E-02	9.76562 E-02
	14.146	2.6949		8.9565	24.571
	12.271	2.4413		7.0000	29.000

REFERENCES

Collections of Mathematical Subroutines, like:

- SSP IBM, Scientific Subroutine Package, Programmers Manual. Copyright International Business Machines Corporation.
 - SPSS, Statistical Package for Social Sciences. Norman H. Nie et al., New York, McGraw Hill Book Company, 2nd edition.
 - BMDP, Biomedical Computer Programs (W. J. Dixon, Ed.). Berkeley. University of California Press.
- Cooley, W. W., and P. R. Lohnes, 1973: *Multivariate Data Analysis*. New York, John Wiley & Sons.
- Diday, E., 1974: *Optimization in Non-Hierarchical Clustering*. In: *Pattern Recognition*, Vol. 6, Pergamon Press: 17—33.
- Good, W., 1980: *Structural Investigations of Snow*. In: *Pattern Recognition in Practice*. (E. S. Gelsema and L. N. Kanal, Eds.) North Holland Publishing Company: 161—170.
- Lebart, L., and P. Fenelon, 1973: *Statistique et Informatique Appliquées*. Paris, Dunod, 2nd edition.
- Oerter, H., 1981: *Untersuchungen über das Abflußverhalten aus dem Vernagtferner unter besonderer Berücksichtigung des Schmelzwasserabflusses im Firnkörper*. Gesellschaft für Strahlen- und Umweltforschung mbH, München. GSF-Bericht, R 267.
- Oerter, H., O. Reinwarth and H. Rufli, 1982: *Core drilling through a temperate alpine glacier (Vernagtferner, Oetztal Alps) in 1979*. *Z. Gletscherk. Glazialgeol.* 18 (1): 1—11 (in this volume).
- Schotterer, U., W. Haeberli, W. Good, H. Oeschger and H. Röthlisberger, 1978: *Datierung von kaltem Firn und Eis in einem Bohrkern von Colle Gnifetti, Monte Rosa*. In: *Gletscher und Klima*, Jb. Schweiz. Naturf. Ges., wiss. Teil, Basel, Verlag Birkhaeuser: 48—57.
- Spaeth, H., 1975: *Cluster-Analyse Algorithmen*. München, R. Oldenbourg Verlag.
- Underwood, E. E., 1970: *Quantitative Stereology*, Reading, Mass. Addison Wesley Publishing Company.

Manuscript received December 27, 1982

Author's address: Dr. W. Good
 Swiss Federal Institute for Snow and Avalanche Research
 CH-7260 Weissfluhjoch/Davos, Switzerland